

Automatic Medical Image Segmentation Based on Finite Skew Gaussian Mixture Model

Nagesh Vadaparathi¹, Srinivas Yerramalli², Suresh Penumatsa³, and Sitharama Poosapati⁴

^{1,4}Department of Information Technology, MVGR College of Engineering, India

²Department of Information Technology, GIT, GITAM University, India

³Department of Computer Science, Adikavi Nannayya University, India

⁴Department of CSE, MVGR College of Engineering, India

Abstract: A novel methodology for segmenting the brain Magnetic Resonance Imaging (MRI) images using the finite skew Gaussian mixture model has been proposed for improving the effectiveness of the segmentation process. This model includes Gaussian mixture model as a limiting case and we believe does more effective segmentation of both symmetric and asymmetric nature of brain tissues as compared to the existing models. The segmentation is carried out by identifying the initial parameters and utilizing the Expectation-Maximization (EM) algorithm for fine tuning the parameters. For effective segmentation, hierarchical clustering technique is utilized. The proposed model has been evaluated on the brain images extracted from the brain web image database using 8 sub-images of 2 brain images. The segmentation evaluation is carried out using objective evaluation criterion viz. Jacquard Coefficient (JC) and Volumetric Similarity (VS). The performance evaluation of reconstructed images is carried out using image quality metrics. The experimentation is carried out using T_1 weighted images and the results are presented. We infer from the results that the proposed model achieves good segmentation results when used in brain image processing.

Keywords: Segmentation, skew Gaussian mixture model, objective evaluation, image quality metrics, EM algorithm.

Received September 13, 2012; accepted March 4, 2013; published online October 29, 2015

1. Introduction

Medical imaging is a process of using specialized instruments and technique by extracting the relevant information about the internal biological structure and the functions of the body. Medical imaging is considered a part of radiological science because of the fact that most of the diagnosing requirements available today are based on radiology. Among the various techniques available for extracting the medical images, Magnetic Resonance Imaging (MRI) has gained an edge due to the non-ionizing radiation that is used in this process. Quite a lot of literature exists on medical image processing related to identification of various abnormalities in body scans, including medical conditions related to brain. Diagnosis of medical conditions of brain and their precise treatment would need segmentation of brain anatomical structure to differentiate tissues CSF, WM and GM.

A challenge in image segmentation here is to differentiate the ventricle, brain and the brain tumour made complicated by the convoluted shape, inhomogeneous intensities, noise and low intensity ranges [10]. This challenge has inspired the development of latest technologies that are robust in identifying the diseases, to differentiate the brain structure and helping out in identifying the diseases. A number of medical image segmentation techniques have been proposed in the literature ranging from threshold based, edge based, region based

techniques [19] and mixture models [2, 8, 16, 22]. Among these techniques, mixture models have gained popularity due to the fact that, while segmenting the medical images, it involves the parameters into consideration which results in effective partitioning. Most of the techniques based on mixture models are Gaussian mixture model based. This is due to the fact that most of the statistical methods rely on Gaussian mixture assumptions for the classification of the brain tissues CSF, WM and GM. It is also assumed that the shapes of the histogram of these tissues are symmetric in nature and hence, Gaussian mixture models can be a better choice [12].

But, in practicality, the tissues are both left skewed and right skewed [3, 9] and hence, symmetric distribution cannot effectively segment the tissues. Also, due to the limited image resolution, the pixels at the boundaries cannot be segmented effectively while considering the Gaussian mixture model and this may lead to partial volume effect where one brain tissue may contain more than one tissue type. In order to overcome these disadvantages of the Gaussian mixture model, it is needed to consider the variations of Gaussian mixture model. Therefore, in this paper, skew Gaussian mixture model is utilized which includes Gaussian mixture model as a particular case. Skew Gaussian mixture model is preferred over the other asymmetric models such as gamma, log normal

because of the fact that in the multivariate case, the multivariate becomes intricate, and also as we depart from symmetry, skew Gaussian tends to Gaussian distribution. In order to, carry out the proposed work, we have considered the data sets of the brain images from brainweb images. The advantages of using the brainweb database are that the comparison can be made available using the ground truth for the tissue classes (CSF, WM and GM) from which the digital phantom were created [21].

The segmentation evaluation is carried out by using objective evaluation technique such as Volumetric Similarity (VS), Jacquard Index. The retrieval of the image is done by the segmentation algorithm and the performance of the output obtained is evaluated using image quality metrics proposed by [6]. To segment any image, first we have to divide the image into K clusters. Many researchers have utilized K-Means algorithm for this purpose [11, 15], but the main disadvantage with regard to K-Means algorithm is that it does not necessarily find the most optimal configuration and it is also sensitive to initial randomly selected segment centres. To overcome this disadvantage, hierarchical clustering algorithm is utilized in this paper. The initial estimates obtained by hierarchical clustering are refined by using Expectation-Maximization (EM) algorithm presented in section 5 of the paper. The paper is organized as follows: Section 2 deals with introduction to hierarchical clustering. Section 3 deals with skew Gaussian distribution, initialization of parameters are discussed in section 4 and updating of initial estimates is presented in section 5. The experimentation is carried out with 8 sub-images of 2 different brain medical images and the results are tabulated.

2. Hierarchical Clustering Algorithm

The first step in any segmentation algorithm is to divide image into different image regions. Many segmentation algorithms are presented in literature [5, 11, 13, 14, 17]. Among these techniques, medical image segmentation based on K-Means is mostly utilized [11, 15]. But, the main disadvantage with K-Means is that, K-Means are slow in convergence and pseudo unsupervised learning that requires the initial value of K . Hence, in this paper we have used hierarchical clustering algorithm in order to identify the initial clusters. The advantages of the hierarchical algorithm [1, 4] are as stated below:

- Embedded flexibility regarding a level of granularity.
- Ease of handling of any forms of similarity or distance.
- Consequently applicability to any attributes types.
- Hierarchical clustering algorithms are more versatile.

The algorithm for hierarchical clustering is presented below.

A hierarchical clustering goes one step further by collecting similar clusters at different levels into a single cluster by forming a tree which gives better selection of clusters for further exploration and hence, in this method hierarchical clustering is utilized.

Given a set of N items to be segmented and an $M \times N$ distance (or similarity) matrix, the basic process of hierarchical segmenting is as follows:

1. Assign each item to a segment, so that, if we have N items, it implies that we have N segments, each containing just one item. Let the distances (similarities) between the segments be the same as those (similarities) between the items they contain.
2. Find the closest (most similar) pair of segments and merge them into a single segment, i.e., we will now have one segment less.
3. Compute distances (similarities) between the new segment and each of the old segments.
4. Repeat steps 2 and 3 until all items are segmented into a single segment of size N .

Step 3 can be done using single-linkage method. In single-linkage segmenting also, called the connectedness or minimum method, we consider the between one segment and another to be equal to the shortest distance from any member of one segment to any member of the other segment. If the data consist of similarities, we consider the similarity between one segment and another to be equal to the greatest similarity from any member of one segment to any member of the other segment. The $M \times N$ proximity matrix is $D=[d(i, j)]$. The segmenting is assigned sequence numbers $0, 1, \dots, (n-1)$ and $L(k)$ is the level of the k th segmenting. A segment with sequence number m is denoted as (m) and the proximity between segments (r) and (s) is denoted as $d[(r), (s)]$. Algorithm 1 is composed of the following steps:

Algorithm 1: Single linkage.

1. Start with the disjoint segments having level $L(0)=0$ and sequence number $m=0$.
2. Find the least dissimilar pair of segments in the current s , say pair $(r), (s)$, where the minimum is over all pairs of segments in the current segmenting.
3. Increment the sequence number: $m=m+1$. Merge segments (r) and (s) into a single segment to form the next segmenting m . Set the level of this segmenting to $L(m)=d[(r), (s)]$.
4. Update the proximity matrix, D by deleting the rows and columns corresponding to segments (r) and (s) and adding a row and column corresponding to the newly formed segment. The proximity between the new segment, denoted (r, s) and the old segment (k) is defined as $d[(k), (r, s)]=\min(d[(k), (r)], d[(k), (s)])$.
5. If all objects are in one segment, stop. Else, go to step.2

3. Skew Gaussian Distribution

The pixels intensities inside the medical images may not be symmetric or bell shaped due to several factors associated like part of the body, bone structure etc. In these cases, the pixels are distributed asymmetrically and follow a skew distribution. Hence, to categorize these sorts of medical images, skew Gaussian distribution is well suited. Every image is a collection of several regions. To model the pixel intensities inside these image regions, we assume that the pixels in each region follow a skew normal distribution, where the probability density function is given by:

$$f(z) = 2 \cdot \phi(z) \cdot \Phi(\alpha z); \quad -\infty < z < \infty \quad (1)$$

Where

$$\Phi(\alpha z) = \int_{-\infty}^{\mu z} \phi(t) dt \quad (2)$$

And

$$\phi(z) = \frac{e^{-\frac{1}{2}z^2}}{\sqrt{2\pi}} \quad (3)$$

Let, $y = \mu + \sigma z$.

$$z = \left(\frac{y - \mu}{\sigma} \right) \quad (4)$$

Substituting Equations 2, 3 and 4 in Equation 1.

$$f(z) = \sqrt{\frac{2}{\pi}} \cdot e^{-\frac{1}{2} \left(\frac{y - \mu}{\sigma} \right)^2} \left[\alpha \left(\frac{y - \mu}{\sigma} \right) \int_{-\infty}^{\frac{1}{2} \left(\frac{y - \mu}{\sigma} \right)^2} \frac{e^{-\frac{1}{2} \left(\frac{t - \mu}{\sigma} \right)^2}}{\sqrt{2\pi}} dt \right] \quad (5)$$

4. Initialization of Parameters

In order to, initialize the parameters, it is needed to obtain the initial values of the model distribution. The initial estimates of the Mixture model μ_i , σ_i and α_i where $i=1, 2, \dots, k$ are estimated using Hierarchical Clustering algorithm as proposed in section 2. It is assumed that the pixel intensities of the entire image is segmented into a K component model π_i , $i=1, 2, \dots, K$ with the assumption that $\pi_i=1/K$ where K is the value obtained from hierarchical clustering algorithm discussed in section 2.

5. Updation of Initial Estimates through EM Algorithm

The initial estimates of μ_i^{l+1} , σ_i^{l+1} , α_i^{l+1} that are obtained from section 4 are to be refined to obtain the final estimates. For this purpose EM algorithm is utilized. The EM algorithm consists of 2 steps E-step and M-step. In the E-step, the initial estimates obtained in section 4 are taken as input and the final updated equations are obtained in the M-step. The updated equations for the model parameters μ , σ and α are given below:

$$\mu^{(l+1)} = y + \sigma^{(l)} + \frac{1}{\alpha^{(l)} \left(\frac{y - \mu^{(l)}}{\sigma^{(l)}} \right) \int_{-\infty}^{\frac{1}{2} \left(\frac{y - \mu^{(l)}}{\sigma^{(l)}} \right)^2} e^{-\frac{1}{2} \left(\frac{t - \mu^{(l)}}{\sigma^{(l)}} \right)^2} dt} \quad (6)$$

$$\sigma^{(l)} \left(\frac{y - \mu^{(l)}}{\sigma^{(l)}} \right) \int_{-\infty}^{\frac{1}{2} \left(\frac{y - \mu^{(l)}}{\sigma^{(l)}} \right)^2} (t - \mu^{(l)}) e^{-\frac{1}{2} \left(\frac{t - \mu^{(l)}}{\sigma^{(l)}} \right)^2} dt - \sigma^{(l)} \alpha^{(l)} e^{\left(\frac{\left[\left(\alpha^{(l)} + \sigma^{(l)} \right) \mu^{(l)} - \alpha^{(l)} y \right]^2}{2\sigma^{(l)}} \right)}$$

$$\sigma^{(l+1)} = \frac{1}{\left[\frac{y - \mu^{(l)}}{\sigma^{(l)}} + \frac{1}{\alpha^{(l)} \left(\frac{y - \mu^{(l)}}{\sigma^{(l)}} \right) \int_{-\infty}^{\frac{1}{2} \left(\frac{y - \mu^{(l)}}{\sigma^{(l)}} \right)^2} e^{-\frac{1}{2} \left(\frac{t - \mu^{(l)}}{\sigma^{(l)}} \right)^2} dt} + \alpha^{(l)} \left(\frac{y - \mu^{(l)}}{\sigma^{(l)}} \right) \int_{-\infty}^{\frac{1}{2} \left(\frac{y - \mu^{(l)}}{\sigma^{(l)}} \right)^2} e^{-\frac{1}{2} \left(\frac{t - \mu^{(l)}}{\sigma^{(l)}} \right)^2} dt + \alpha^{(l)} \left(\frac{y - \mu^{(l)}}{\sigma^{(l)}} \right) \int_{-\infty}^{\frac{1}{2} \left(\frac{y - \mu^{(l)}}{\sigma^{(l)}} \right)^2} e^{-\frac{1}{2} \left(\frac{t - \mu^{(l)}}{\sigma^{(l)}} \right)^2} dt \right]} \left[\frac{\left[\left(\alpha^{(l)} + \sigma^{(l)} \right) \mu^{(l)} - \alpha^{(l)} y \right]^2}{2\sigma^{(l)}} \right] \quad (7)$$

$$\alpha^{(l+1)} = \frac{\sqrt{2} \sigma^{(l)}}{\mu^{(l)} - y} \left[\log \left(\frac{\alpha^{(l)} \left(\frac{y - \mu^{(l)}}{\sigma^{(l)}} \right) \int_{-\infty}^{\frac{1}{2} \left(\frac{y - \mu^{(l)}}{\sigma^{(l)}} \right)^2} e^{-\frac{1}{2} \left(\frac{t - \mu^{(l)}}{\sigma^{(l)}} \right)^2} dt - \log \left(\frac{y - \mu^{(l)}}{\sigma^{(l)}} \right)} \right) \right]^{\frac{1}{2}} - \frac{\sigma^{(l)} \mu^{(l)}}{\mu^{(l)} - y} \quad (8)$$

6. Segmentation Algorithm

After refining the parameters, the first step in image reconstruction by allocating pixels to the segments. This operation is done by Algorithm 2. The segmentation algorithm consists of 7 steps.

Algorithm 2: Segmentation algorithm.

- Step 1: Obtain the pixel intensities of the gray image. Let they be represented by x_{ij} .
- Step 2: Obtain the number of regions by hierarchical clustering algorithm and divide the (image) pixel into regions.
- Step 3: For each region obtain the initial estimates using moment methods of estimation for μ_i , σ_i . Let $\alpha_i=1/k$ be the initial estimate for α_i .
- Step 4: Obtain the refined estimates of μ_i , σ_i , α_i for $i=1 \dots k$ using updated equations for the parameters derived by EM algorithm with step 3 estimates as initial estimates.
- Step 5: Implement the segmentation and retrieval algorithm by considering maximum Likelihood estimate.
- Step 6: With the step 5 obtain the image quality metric.
- Step 7: The image segmentation is carried out by assigning each pixel into a proper region (Segment) according to maximum likelihood estimates of the j^{th} element L_j according to the following equation:

$$L_j = \text{Max}_j \left\{ \sqrt{\frac{2}{\pi}} e^{-\frac{1}{2} \left(\frac{y - \mu}{\sigma} \right)^2} \left[\alpha \left(\frac{y - \mu}{\sigma} \right) \int_{-\infty}^{\frac{1}{2} \left(\frac{y - \mu}{\sigma} \right)^2} \frac{e^{-\frac{1}{2} \left(\frac{t - \mu}{\sigma} \right)^2}}{\sqrt{2\pi}} dt \right] \right\} \quad (9)$$

7. Experimental Results and Performance Evaluation

After developing the segmentation algorithm, the algorithm is applied to 8 sub images of 2 T_1 -weighted different brain medical images obtained from the brainweb database of dimensions 150×174 and 163×199 respectively. The segmentation performance is evaluated by using objective segmentation

evaluation criteria based on *Jacquard Index* and *VS* using formula:

$$Jacquard\ Quotient = \frac{|X \cap Y|}{|X \cup Y|} = \frac{a}{a + b + c} \tag{10}$$

$$VS = 1 - \frac{||X| - |Y||}{|X| + |Y|} = 1 - \frac{|b - c|}{2a + b + c} \tag{11}$$

Where $a = |X \cap Y|$, $b = \left| \frac{X}{Y} \right|$, $c = \left| \frac{Y}{X} \right|$, $d = |X \cup Y|$ and the results obtained are tabulated in Table 1 and Figure 1 and the same is depicted using Figure 2.

Table 1. Segmentation metrics.

Image	Quality Metric	GMM	Skew GMM with k-Means	Skew GMM with Hierarchical Clustering	Standard Limits	Standard Criteria
B0S1	Jacquard quotient	0.089	0.689	0.703	0 to 1	Close to 1
	Volume Similarity	0.432	0.733	0.8799	0 to 1	Close to 1
B0S2	Jacquard quotient	0.0677	0.7656	0.7921	0 to 1	Close to 1
	Volume Similarity	0.3212	0.8767	0.8814	0 to 1	Close to 1
B0S3	Jacquard quotient	0.0434	0.6567	0.7143	0 to 1	Close to 1
	Volume Similarity	0.123	0.812	0.916	0 to 1	Close to 1
B0S4	Jacquard quotient	0.0456	0.7878	0.874	0 to 1	Close to 1
	Volume Similarity	0.2233	0.3232	0.54	0 to 1	Close to 1
B1S1	Jacquard quotient	0.141	0.776	0.791	0 to 1	Close to 1
	Volume Similarity	0.313	0.397	0.784	0 to 1	Close to 1
B1S2	Jacquard quotient	0.098	0.7892	0.877	0 to 1	Close to 1
	Volume Similarity	0.04334	0.878	0.881	0 to 1	Close to 1
B1S3	Jacquard quotient	0.0222	0.8926	0.9124	0 to 1	Close to 1
	Volume Similarity	0.3223	0.3429	0.3543	0 to 1	Close to 1
B1S4	Jacquard quotient	0.455	0.762	0.815	0 to 1	Close to 1
	Volume Similarity	0.329	0.7001	0.7158	0 to 1	Close to 1

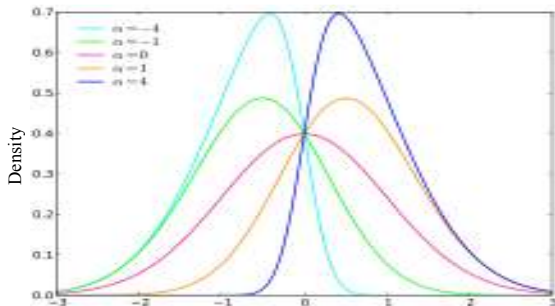


Figure 1. Frequency curves of skew normal distributions.

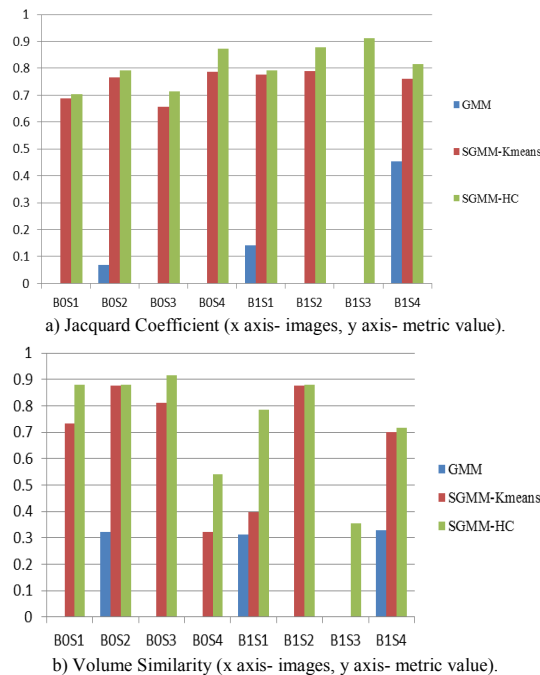


Figure 2. Comparisons of segmentation techniques.

In order to, demonstrate the algorithm, the initial number of segments of the medical images under consideration is obtained from the histograms of the respective image and is presented in Table 2.

Table 2. Initial estimates of K (By histogram).

Image	B0	B1
Estimation for K	4	3

After obtaining the initial estimates, hierarchical clustering is applied for obtaining initial estimates of model parameters and initial estimates of number of segments for each of medical image and is presented in Table 3.

Table 3. Estimates of hierarchical clustering.

Image	B0	B1
Estimate of Hierarchical Clustering	4	4

After obtaining the initial estimates, the equations for EM algorithm are derived and the final parameters are estimated and are presented in Table 4.

Table 4. Estimation of initial and final parameters.

Image	Regions (i)	Estimation of Initial Parameters			Estimation of Final Parameters using EM Algorithm		
		Number of Image Regions, k=4			Number of Image Regions, k=4		
		μ_i	σ_i	α_i	μ_i'	σ_i'	α_i'
B0	S1	6.7126	10.247	0.3	0.0865	0.821	0.3
	S2	61.73	16.89	0.3	0.0002	0.004	0.3
	S3	123.55	22.37	0.2	6.41e-05	0.0024	0.2
	S4	214.59	24.97	0.2	4.421e-05	0.0013	0.2
B1	S1	3.64	8.23	0.3	-0.4891	0.949	0.3
	S2	51.08	16.31	0.3	8.203e-11	1.16e-09	0.3
	S3	115.46	18.62	0.2	6.512e-11	9.05e-10	0.2
	S4	179.8	24.86	0.2	3.3022	13.198	0.2

After obtaining the updated estimates, using these estimates the image reconstruction is carried out by assigning each pixel in the PDF of the image and the outputs obtained are presented in Figure 3.

The image reconstruction is carried out by assigning each pixel to the segments using the segmentation algorithm and the probability density function and is given as follows:

$$f(z) = \sqrt{\frac{2}{\pi}} e^{-\frac{1}{2} \left(\frac{y-\mu}{\sigma} \right)^2} \left[\int_{-\infty}^{\alpha \left(\frac{y-\mu}{\sigma} \right)} e^{-\frac{1}{2} \left(\frac{t-\mu}{\sigma} \right)^2} dt \right] \tag{12}$$

After reconstructing the image, the reconstructed images are shown in Figure 3.

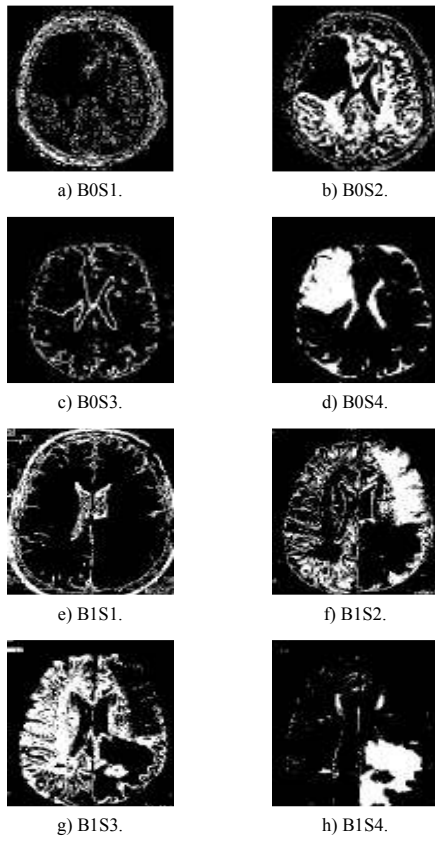


Figure 3. Reconstructed images of image B0 and B1.

The input images for the above reconstructed images B0 and B1 are shown in Figure 4.

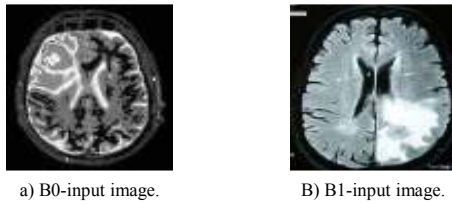


Figure 4. Input images of image B0 and B1.

In order to, evaluate the performance of the reconstructed image, image quality metrics are used and the metrics utilized for this purpose are presented in Table 5.

Table 5. Formulae for evaluating quality metrics used.

Quality Metric	Formula to Evaluate
Average Difference	$\frac{\sum_{j=1}^M \sum_{k=1}^N [F(j, k) - \hat{F}(j, k)]}{MN}$ Where M, N are image matrix rows and columns
Maximum Distance	$Max \left[\left F(j, k) - \hat{F}(j, k) \right \right]$
Image Fidelity	$1 - \frac{\sum_{j=1}^M \sum_{k=1}^N [F(j, k) - \hat{F}(j, k)]}{\sum_{j=1}^M \sum_{k=1}^N [F(j, k)]^2}$ Where M, N are image matrix rows and columns
Mean Squared Error	$\frac{1}{MN} \left[\sum_{j=1}^M \sum_{k=1}^N \left[O \{ F(j, k) - O \{ \hat{F}(j, k) \} \right]^2 \right] / \sum_{j=1}^M \sum_{k=1}^N [O \{ F(j, k) \}]^2$ Where M, N are image matrix rows and columns
Signal to Noise Ratio	$20 \log_{10} \left(\frac{MAX_i}{\sqrt{MSE}} \right)$ Where, MAX_i is maximum possible pixel value of image, Mean Squared Error (MSE) is the

Using above metrics, the performance evaluation is carried out and the comparison is done with respect to the model proposed using skew symmetric distribution [15] and the results are presented in Table 5 and Figure 5.

Table 6. Quality measures.

Image	Quality Metric	GMM	Skew GMM with K-Means	Skew GMM with Hierarchical Clustering	Standard Limits	Standard Criteria
	Average Difference	0.573	0.773	0.812	-1 to 1	Closer to 1
	Maximum Distance	0.422	0.922	0.9325	-1 to 1	Closer to 1
	Image Fidelity	0.416	0.875	0.923	0 to 1	Closer to 1
	Mean Squared error	0.04	0.134	0.094	0 to 1	Closer to 0
	Signal to noise ratio	17.41	29.23	33.89	$-\infty$ to ∞	As big as Possible
	Average Difference	0.37	0.876	0.749	-1 to 1	Closer to 1
	Maximum Distance	0.221	0.897	0.912	-1 to 1	Closer to 1
	Image Fidelity	0.336	0.876	0.859	0 to 1	Closer to 1
	Mean Squared error	0.2404	0.211	0.2019	0 to 1	Closer to 0
	Signal to noise ratio	14.45	35.65	39.85	$-\infty$ to ∞	As big as Possible
	Average Difference	0.456	0.76	0.81	-1 to 1	Closer to 1
	Maximum Distance	0.345	0.879	0.807	-1 to 1	Closer to 1
	Image Fidelity	0.44	0.86	0.917	0 to 1	Closer to 1
	Mean Squared error	0.22	0.23	0.2123	0 to 1	Closer to 0
	Signal to noise ratio	19.88	37.98	39.71	$-\infty$ to ∞	As big as Possible
	Average Difference	0.231	0.473	0.4991	-1 to 1	Closer to 1
	Maximum Distance	0.224	0.977	0.971	-1 to 1	Closer to 1
	Image Fidelity	0.212	0.813	0.892	0 to 1	Closer to 1
	Mean Squared error	0.24	0.121	0.1192	0 to 1	Closer to 0
	Signal to noise ratio	21.42	33.28	37.41	$-\infty$ to ∞	As big as Possible
	Average Difference	0.342	0.764	0.7015	-1 to 1	Closer to 1
	Maximum Distance	0.317	0.819	0.854	-1 to 1	Closer to 1
	Image Fidelity	0.391	0.812	0.876	0 to 1	Closer to 1
	Mean Squared error	0.2514	0.228	0.1759	0 to 1	Closer to 0
	Signal to noise ratio	3.241	5.514	5.68	$-\infty$ to ∞	As big as Possible
	Average Difference	0.21	0.3653	0.232	-1 to 1	Closer to 1
	Maximum Distance	0.21	0.892	0.912	-1 to 1	Closer to 1
	Image Fidelity	0.2134	0.787	0.791	0 to 1	Closer to 1
	Mean Squared error	0.06	0.145	0.594	0 to 1	Closer to 0
	Signal to noise ratio	13.43	49.22	20.39	$-\infty$ to ∞	As big as Possible
	Average Difference	0.3232	0.322	0.4592	-1 to 1	Closer to 1
	Maximum Distance	0.123	0.212	0.456	-1 to 1	Closer to 1
	Image Fidelity	0.233	0.897	0.923	0 to 1	Closer to 1
	Mean Squared error	0.01	0.4345	0.119	0 to 1	Closer to 0
	Signal to noise ratio	11.11	27.267	29.86	$-\infty$ to ∞	As big as Possible
	Average Difference	0.314	0.338	0.497	-1 to 1	Closer to 1
	Maximum Distance	0.241	0.249	0.317	-1 to 1	Closer to 1
	Image Fidelity	0.293	0.683	0.791	0 to 1	Closer to 1
	Mean Squared error	0.18	0.197	0.213	0 to 1	Closer to 0
	Signal to noise ratio	21.214	78.19	99	$-\infty$ to ∞	As big as Possible

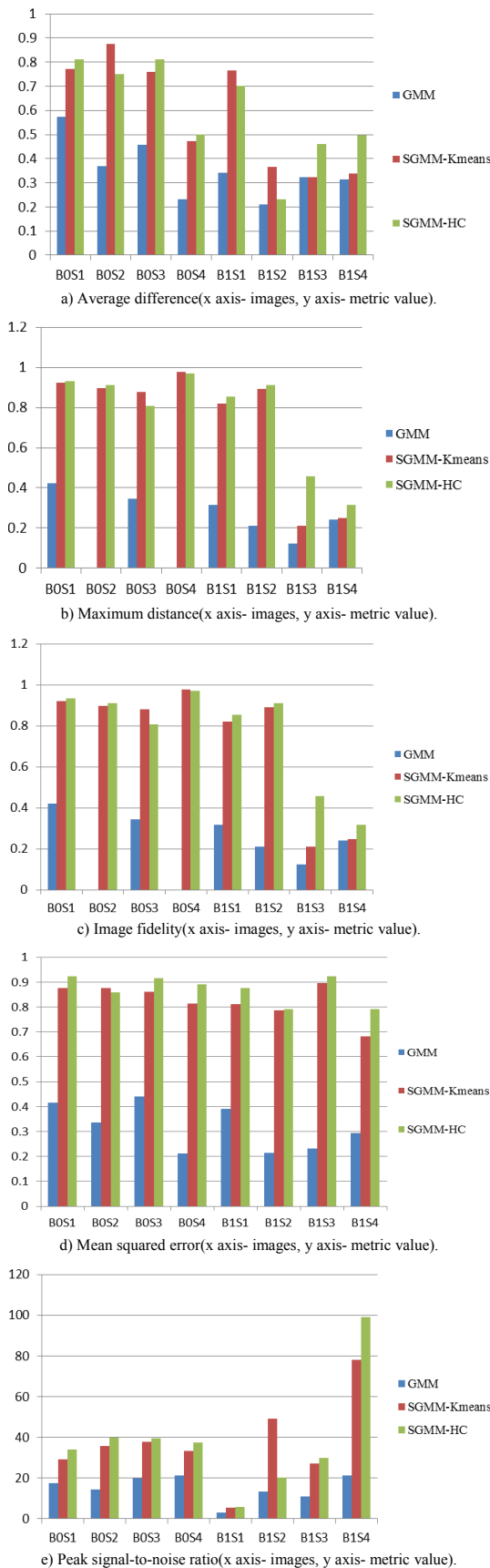


Figure 5. Comparisons of techniques.

From the above Table 6 and Figure 5, it can be clearly seen that the model developed by using hierarchical clustering shows better results with respect to the quality metrics. The model is compared the existing models based on Gaussian mixture model and

skew Gaussian mixture model with K-Means algorithm and the results are shown pictorially by Figure 2 and Figure 5.

From the above graphs, it can be clearly seen that the model developed by using hierarchical clustering performs better compared to the earlier models. This may be due to the fact of the asymmetric nature of the medical images.

8. Conclusions

A medical image segmentation technique based on finite skew Gaussian mixture model with hierarchical clustering using EM algorithm is developed and evaluated. The results obtained by this algorithm outperform the existing methods. This method can be mainly suited in particular cases of medical pathology where diseases like acoustic neuronal and Parkinson’s diseases can be identified accurately there by helping in proper diagnosis and preventing disabilities such as hearing loss and preventing disabilities such as hearing loss and dizziness.

References

- [1] Abbas O., “Comparisons between Data Clustering Algorithms,” *The International Arab Journal of Information Technology*, vol. 5, no. 3, pp. 320-325, 2008.
- [2] Adelino R. and Ferreira D., “Bayesian Mixture Models of Variable Dimension for Image Segmentation,” *Computer Methods and Programs in Biomedicine*, vol. 94, no. 1, pp. 1-14, 2009.
- [3] Ashburner J., Friston K., “Multimodal Image Coregistration and Partitioning-A Unified Framework,” *NeuroImage*, vol. 6, no. 3, pp. 209-217, 1997.
- [4] Bouix S, Martin-Fernandez M, Ungar L, Nakamura M., Koo M., McCarley R., and Shenton M., “On Evaluating Brain Tissue Classifiers without a Ground Truth,” *Journal of NeuroImage*, vol. 36, no. 4, pp. 1207-1224, 2007.
- [5] Dugas-Phocion G., Ballester M., Malandain G., Ayache N., “Improved EM-based Tissue Segmentation Andpartial Volume Effect Quantification in Multi-Sequence Brain MRI,” in *Proceedings of the 7th International Conference*, Saint-Malo, France, pp. 26-33, 2004.
- [6] Eskicioglu A. and Fisher, P., “Image Quality Measures and Their Performance,” *IEEE Transactions on Communications*, vol. 43, no. 12, pp. 2959-2965, 1995.
- [7] Greggio N., Bernardino A., Laschi C., Dario P., and Santos-Victor J., “Fast Estimation of Gaussian Mixture Models for Image Segmentation,” *Machine Vision and Applications*, vol. 23, no. 4, pp. 773-789, 2011.

- [8] Guang J., Xia Y., Yanning Z., and Dagan F., "Hybrid Genetic and Variational Expectation-Maximization Algorithm for Gaussian-Mixture-Model-Based Brain MR Image Segmentation," *IEEE Transactions on Information Technology in Biomedicine*, vol. 15, no. 3, pp. 373-380, 2011.
- [9] Hartigan J., *Clustering Algorithms*, New York: Wiley, 1975.
- [10] Heng-Hua C., Daniel J., Gary R., and Arthur W., "Segmentation of Brain MR Images using a Charged Fluid Model," *IEEE Transactions on Biomedical Engineering*, vol. 54, no. 10, pp. 1798-1813, 2007.
- [11] Kalaiselvi T., Somasundaram K., and Rajeswari M., "Fast Brain Abnormality Detection Method for Magnetic Resonance Images (MRI) of Human Head Scans Using K-Means Clustering Technique," in *Proceedings of the 4th International Conference on Signal and Image Processing 2012*, pp. 225-234, 2013.
- [12] Lee J., Su H., Cheng P., Liou M., Aston J., Tsai A., and Chen C., "MR Image Segmentation Using a Power Transformation Approach," *IEEE Transactions on Medical Imaging*, vol. 28, no. 6, pp. 894-905, 2009.
- [13] Leemput K., Maes F., Vandermeulen D., and Suetens P., "A Unifying Framework for Partial Volume Segmentation of Brain MR Images," *IEEE Transactions On Medical Imaging*, vol. 22, no. 1, pp. 105-119, 2003.
- [14] Leemput K., Maes F., Vandermeulen D., and Suetens P., "Automated Model-based Tissue Classification of MR Images of the Brain," *IEEE Transactions on Medical Imaging*, vol. 18, no. 10, pp. 897-908, 1999.
- [15] Nagesh V., Srinivas Y., and Suresh Varma P., "Unsupervised Medical Image Segmentation on Brain MRI images using Skew Gaussian Distribution," in *Proceedings of International Conference on Recent Trends in Information Technology*, Chennai, Tamil Nadu, pp.1293-1297, 2011.
- [16] Nguyen T. and Wu J., "Robust Student's-t Mixture Model with Spatial Constraints and Its Application in Medical Image Segmentation," *IEEE Transactions on Medical Imaging*, vol. 31, no. 1, pp. 103-116, 2011.
- [17] Pham D., Xu C., and Prince J., "A Survey of Current Methods in Medical Image Segmentation," *Annual Review of Biomedical Engineering*, vol. 2, pp. 315-337, 2000.
- [18] Prastawa M., Bullitt M., Ho S., and Gerig G., "Robust Estimation For brain Tumor Segmentation," in *Proceedings of the 6th International Conference*, Canada, pp. 530-537, 2003.
- [19] Bandhyopadhyay S. and Paul T., "Segmentation of Brain MRI Image-A Review," *International Journal of Advanced Research in Computer Science and Software Engineering*, vol. 2, no. 3, , pp.409-413, 2012.
- [20] Shattuck D., Prasad G., Mirza M., Narr K., and Toga A., "Online Resource for Validation of Brain Segmentation Methods," *NeuroImage*, vol. 45, no. 2, pp. 431-439, 2009.
- [21] Tsang O., Gholipour A., Kehtarnavaz N., Gopinath K., Briggs R., and Panahi I., "Comparison of Tissue Segmentation Algorithms in NeuroImage Analysis Software Tools," in *Proceedings of the 30th Annual International IEEE EMBS Conference*, British Columbia, Canada, pp. 3924-3928, 2008.
- [22] Xiao Y, Shah M, Francis S, Arnold D., Arbel T and Collins D., "Optimal Gaussian Mixture Models of Tissue Intensities in Brain MRI of Patients with Multiple-Sclerosis," in *Proceedings of the 1st International Workshop, MLMI 2010, Held in Conjunction with MICCAI 2010*, Beijing, China, pp. 165-173, 2010.



Nagesh Vadaparathi is working as a professor in Department of Information Technology, MVGR College of Engineering, Vizianagaram, Andhra Pradesh, India. He has about 12 years of teaching experience and his areas of interests include communication networks and protocols, grid computing and bioinformatics apart from image processing. He has published several research papers in various National and International conferences and journals. He is a member of IEEE, IAENG, IACSIT, IIE, CSI and ISTE.



Srinivas Yerramalli is a Professor in Department of Information Technology, GITAM University, Visakhapatnam, India and has about 17 years of teaching experience. His areas of interests include speech processing, data mining, and software reusability apart from image processing. He is having more than 60 publications at national and International level. He is the author for 4 books and a life member of ISTE, CSI, IE, ISTAM, IISA and ISPS.



Suresh Penumatsa is a Professor in Department of Computer Science and Principal of Adikavi Nannaya University, Rajahmundry, India. He is having 17 years of teaching experience. His areas of interests include communication networks, image processing and speech processing. He has published several research papers. He is a life member of ISTE, SMORSI, ISCA and IISA.



Sitharama Poosapati is a Professor in Department of Information Technology, MVGR College of Engineering, Vizianagaram, Andhra Pradesh, India. He has 15 years of Industrial and teaching experience. His areas of interests include distributed computing and computer architecture. He has published several research papers. He is a life member of CSI.